Published in final edited form as:
Nanomedicine. 2011 October ; 7(5): 588–594. doi:10.1016/j.nano.2011.01.008.

Polystyrene nanoparticle trafficking across MDCK-II

Farnoosh Fazlollahi, MS[1,8,*], **Susanne Angelow, PhD**[2,5], **Nazanin R. Yacobi, PhD**[1,8], **Ronald Marchelletta, PhD**[6], **Alan S.L. Yu, PhD**[2,5], **Sarah F. Hamm-Alvarez, PhD**[6], **Zea Borok, MD**[1,2,3,†], **Kwang-Jin Kim, PhD**[1,2,5,6,7], and **Edward D. Crandall, PhD, MD**[1,2,4,8,‡]

[1] Will Rogers Institute Pulmonary Research Center, University of Southern California, Los Angeles, CA, USA

[2] Department of Medicine, University of Southern California, Los Angeles, CA, USA

[3] Department of Biochemistry and Molecular Biology, University of Southern California, Los Angeles, CA, USA

[4] Department of Pathology, University of Southern California, Los Angeles, CA, USA

[5] Department of Physiology and Biophysics, University of Southern California, Los Angeles, CA, USA

[6] Department of Pharmacology and Pharmaceutical Sciences, University of Southern California, Los Angeles, CA, USA

[7] Department of Biomedical Engineering, University of Southern California, Los Angeles, CA, USA

[8] Mork Family Department of Chemical Engineering and Materials Science, University of Southern California, Los Angeles, CA, USA

Abstract

Polystyrene nanoparticles (PNP) cross rat alveolar epithelial cell monolayers via non-endocytic transcellular pathways. To evaluate epithelial cell type-specificity of PNP trafficking, we studied PNP flux across Madin Darby canine kidney cell II monolayers (MDCK-II). Effects of calcium chelation (EGTA), energy depletion (sodium azide (NaN_3) or decreased temperature), and endocytosis inhibitors methyl-β-cyclodextrin (MBC), monodansylcadaverine and dynasore were determined. Amidine-modified PNP cross MDCK-II 500 times faster than carboxylate-modified PNP. PNP flux did not increase in the presence of EGTA. PNP flux at 4°C and after treatment with NaN_3 decreased 75% and 80%, respectively. MBC exposure did not decrease PNP flux, whereas dansylcadaverine- or dynasore-treated MDCK-II exhibited ~80% decreases in PNP flux. Confocal laser scanning microscopy revealed intracellular colocalization of PNP with clathrin heavy chain. These data indicate that PNP translocation across MDCK-II (1) occurs via clathrin-mediated endocytosis and (2) is dependent upon PNP physicochemical properties. We conclude that uptake/trafficking of nanoparticles into/across epithelia is dependent both on properties of the nanoparticles and the specific epithelial cell type.

[*]To whom correspondence should be addressed: Farnoosh Fazlollahi, M.S., Department of Medicine, University of Southern California, HMR 914, 2011 Zonal Avenue, Los Angeles, CA 90033, USA, Office: 323 442-1217, Fax: 323 226-2899, fazlolla@usc.edu.
[†]Z. Borok is Ralph Edgington Chair in Medicine.
[‡]E. D. Crandall is Hastings Professor and Kenneth T. Norris Jr. Chair of Medicine.

Keywords

epithelial transport; endocytosis; clathrin; dynamin; surface charge

Background

Nanoparticles (NP) are defined as particles with at least one dimension <100 nm. Small size, large surface area, high surface reactivity and composition-dependent characteristics of NP are uniquely suited for various nanoscale operations [1,2,3]. Engineered NP are promising candidates for therapeutic and diagnostic applications in biomedicine (e.g., highly sensitive and stable probes to detect changes in intracellular molecules [4], early detection and diagnosis [5], and targeted delivery of therapeutics to specific cell types [4,5]), although some NP exhibit cellular toxicity [3,6]. Internalization of NP into cells can take place via endocytic and/or non-endocytic pathways [7,8,9,10,11]. It has been reported that uptake of NP into cells is influenced by surface charge and size of NP [8,9,12,13,14]. Understanding mechanisms of NP interactions with cells of interest will help lead to improved design of NP as efficient and safe reporters/carriers for biomedical investigations and interventions [8].

Our laboratory recently reported the trafficking profile of polystyrene NP (PNP) with variable size and surface charge across primary cultured rat alveolar epithelial cell monolayers (RAECM) [13,14]. Trafficking rates of PNP across RAECM are dependent on both surface charge density and size, in that we found (a) ~20–40 times greater flux for positively (vs negatively) charged PNP and (b) larger PNP (100 or 120 nm) cross RAECM ~3–4 times slower than smaller PNP (20 nm) [14]. PNP appear to be translocated across RAECM via non-endocytic transcellular pathways, possibly involving diffusion across the lipid bilayer of cell plasma membranes [13].

In this study, we utilized Madin Darby canine kidney cell line monolayers (MDCK-II) as an alternative epithelial model with which to study characteristics of PNP uptake/trafficking. MDCK-II are thought to represent the epithelial barrier of the renal tubule [15,16]. Effects of size and surface charge density of PNP, and effects of EGTA and inhibitors of endocytosis, on PNP trafficking rates across MDCK-II were investigated. We found that processes likely involved in translocation of PNP across MDCK-II are energy- and surface charge-dependent and, in contrast to PNP trafficking across RAECM, take place via clathrin-mediated endocytosis. These data indicate that characteristics of NP uptake/trafficking across epithelial barriers are both cell type-specific and dependent on NP physicochemical properties.

Methods

Nanoparticles

Fluorescently labeled polystyrene nanoparticles (PNP) were purchased from Thermo Fisher Scientific (Waltham, MA). Carboxylate-modified (COO^-, 20 and 100 nm diameter with −304.3 and −320 μEq/g surface charge, respectively) and amidine-modified ($HNC\text{-}NH^{2+}$, 20 and 120 nm with 80.2 and 39.7 μEq/g surface charge, respectively) PNP were used. Excitation/emission wavelengths for carboxylate- and amidine-modified PNP are 580/605 and 490/515 nm, respectively.

MDCK-II

MDCK-II cells were plated on day 0 onto tissue culture-treated polycarbonate filters (Transwell, 12 mm diameter, 0.4 μm diameter pores, Corning-Costar, Cambridge, MA) at

1.5×10^5 cells/cm^2 and maintained in Dulbecco's modified Eagle's (DME) medium (Thermo Fisher Scientific) with 5% fetal bovine serum (Thermo Fisher Scientific), 200 U/mL penicillin (Sigma, St. Louis, MO), 200 μg/mL streptomycin (Sigma) and 2% L-glutamine (Sigma) at 37°C in a humidified atmosphere of 5% CO_2 + 95% air. Cells were fed every other day starting on day 3 in culture when they form confluent monolayers. A rapid screening device (Millicell-ERS; Millipore, Bedford, MA) was used to check transmonolayer electrical resistance (Rt). Confluent MDCK-II were studied on days 5–7 (Rt ~150 Ωcm^2).

Apical-to-basolateral PNP flux

To measure rates of PNP trafficking across MDCK-II, apical fluid was replaced at t = 0 with fresh culture medium containing various PNP at 176 μg/mL. Apical-to-basolateral (a-b) flux at 37°C was estimated from PNP appearing in basolateral fluid over 24 h. PNP concentrations in downstream fluid were estimated spectrofluorometrically using SpectraMax M2 (Molecular Devices, Sunnyvale, CA). Apical [PNP] was determined at t = 0 and 24 h. [PNP] was calculated using standard curves generated with known concentrations of PNP suspended in culture medium. Flux was calculated as $J = (CV)/S/\Delta t$, where J is flux (a-b) of PNP, C is [PNP] in basolateral fluid at Δt, V is basolateral fluid volume, S is nominal surface area of monolayer (1.13 cm^2) and Δt is length of time for flux measurement.

To determine if decreased tight junctional resistance leads to increased trafficking rates, flux of various PNP was measured in the presence of 2 mM ethylene glycol-bis-(2-aminoethyl)-N,N,N′,N′-tetraacetic acid (EGTA, Sigma) in both apical and basolateral fluids. Monolayers were pretreated with EGTA for 30 min, after which apical fluid was replaced at t = 0 with fresh culture medium containing various PNP at 176 μg/mL and 2 mM EGTA.

To determine effects of metabolic inhibition/energy depletion, flux across MDCK-II was measured at 4°C or in the presence of 10 mM sodium azide (Sigma) [17]. In the latter experiments, MDCK-II were bathed on both sides with culture medium containing sodium azide for 30 min prior to and during apical exposure to 176 μg/mL PNP.

To explore mechanisms of PNP translocation, effects of inhibition of lipid raft-mediated endocytosis (including caveolin-mediated endocytosis) were evaluated using methyl-β-cyclodextrin [18,19], monodansylcadaverine was employed for inhibition of clathrin-mediated endocytosis [20,21,22], and dynasore was used to inhibit dynamin-dependent endocytosis (including both clathrin- and caveolin-mediated endocytosis) [23]. Monolayers were bathed on both sides with culture medium containing 10–200 μM methyl-β-cyclodextrin (Sigma), 200 μM monodansylcadaverine (Sigma) or 80 μM dynasore (Sigma) for 30 min prior to replacing apical fluid at t = 0 with fresh culture medium containing both 176 μg/mL of various PNP and specific endocytosis inhibitors.

Immunofluorescence and confocal laser scanning microscopy

MDCK-II were exposed apically to 176 μg/mL amidine-modified (120 nm) or carboxylate-modified (100 nm) PNP at 37°C for 24 h. Exposed monolayers were washed 3 times with ice-cold phosphate buffered saline (PBS, pH 7.2) and fixed in 3.7% formaldehyde (J.T. Baker, Phillipsburg, NJ) at room temperature for 15 min. Monolayers were then treated with 0.5% Triton X-100 (TX-100, Bio-Rad, Hercules, CA) at room temperature for 15 min, followed by rinsing with PBS and blocking with PBS containing both 5% BSA and 0.2% TX-100 for 1 h at room temperature. Mouse antibody against human zonula occludens-1 (ZO-1, Zymed Laboratories, San Francisco, CA) diluted 1:100 using 1% BSA in PBS was incubated with fixed monolayers at 37°C for 1 h, followed by washing with PBS and further incubating monolayers with secondary antibody (goat anti-mouse antibody conjugated to

Alexa 594 or Alexa 488, Invitrogen) diluted 1:100 using 1% BSA in PBS at 37°C for 1 h. Monolayers were then rinsed with PBS and mounted on microscope slides with mounting medium (containing the nuclear staining dye 4′,6-diamidino-2-phenylindole (DAPI) (Vector, Burlingame, CA)).

For labeling clathrin heavy chain, MDCK-II were fixed and permeablized with ice-cold ethanol at −20°C for 5 min and blocked with PBS containing both 5% BSA and 0.2% TX-100 at room temperature for 1 h. Mouse anti-human clathrin heavy chain antibody (BD Biosciences, San Jose, CA) diluted 1:100 in 1% BSA in PBS was incubated with fixed monolayers for 1 h at 37°C. After washing monolayers 3 times with PBS, secondary antibody (goat anti-mouse antibody labeled with Alexa 488, Invitrogen) in 1% BSA in PBS was incubated with monolayers at 37°C for 1 h. Monolayers were then rinsed with PBS and mounted on microscope slides with mounting medium containing DAPI. Negative controls include: i) monolayers incubated with PNP in the presence of 200 μM dansylcadaverine for 1 h, ii) monolayers not exposed to PNP, and iii) monolayers incubated with a primary or secondary antibody alone. These controls were similarly processed as above. Images were acquired with a Zeiss confocal laser scanning microscope (510 Meta NLO CLSM imaging system, Jena, Germany) equipped with argon and red/green HeNe lasers mounted on a vibration-free table and attached to an incubation chamber.

Data analysis

Data are presented as mean ± standard deviation (n = total number of monolayers). Student's *t*-tests were performed for comparisons of two group means. One-way analysis of variance followed by post-hoc tests based on modified Newman-Keuls procedures was performed for comparisons of more than two group means. $P<0.05$ was considered statistically significant.

Results

Figure 1A shows trafficking rates of amidine-modified (positively charged 20 and 120 nm) and carboxylate-modified (negatively charged 20 and 100 nm) PNP across MDCK-II with apical [PNP] of 176 μg/mL. Trafficking of positively charged PNP is 500 times faster than that for comparably sized but negatively charged PNP. Trafficking rates of smaller (20 nm) PNP across MDCK-II are not significantly different from those of larger (100 and 120 nm) PNP with similar surface charge. Figure 1B shows an expanded view of carboxylate-modified (negatively charged 20 and 100 nm) PNP trafficking rates across MDCK-II.

Confocal photomicrographs (at 1 μm intervals) of MDCK-II exposed apically to 176 μg/mL PNP (amidine-modified 120 nm) for 24 h are shown in Figure 2(A-D). PNP are clearly seen intracellularly. Similar observations were noted with carboxylated-modified 100 nm PNP (data not shown).

Monolayer resistance of MDCK-II decreased >95% in the presence of 2 mM EGTA (which chelates free Ca^{2+} in bathing fluids). Flux of amidine-modified PNP across MDCK-II was not increased in the presence of EGTA (Figure 3). It can be noted that flux of 120 nm amidine modified PNP across MDCK-II was decreased by EGTA treatment, while that of 20 nm amidine-modified PNP did not change. On the other hand, flux of carboxylated (20 and 100 nm) PNP in the presence of EGTA were not significantly different from those observed for control (i.e., EGTA-free) monolayers (data not shown).

Flux of amidine-modified (20 and 120 nm) PNP decreased by ~75% across MDCK-II at 4°C compared to control at 37°C (Figure 3), while carboxylate-modified (20 and 100 nm) PNP flux decreased by ~60% at 4°C compared to control at 37°C (data not shown). When cellular ATP was decreased by treating monolayers with 10 mM NaN_3, flux of positively charged

PNP (20 and 120 nm) decreased by ~80% compared to those of NaN_3-free control (Figure 3).In contrast, flux of carboxylated (20 and 100 nm) PNP measured in the presence of NaN_3 was not significantly different from those observed for control (i.e., in the absence of NaN_3) monolayers. Rt of MDCK-II at 4°C and of NaN_3-treated MDCK-II did not decrease compared to respective controls.

Figure 4 shows flux of amidine-modified PNP (20 and 120 nm) in the presence of 10 μM MBC, 200 μM dansylcadaverine or 80 μM dynasore. Flux of these positively charged PNP did not decrease in the presence of 10–200 μM MBC. Similarly, flux of carboxylated PNP (20 and 100 nm) measured in the presence of MBC was not significantly different from those observed in the absence of MBC (data not shown). Rt of MDCK-II treated with MBC decreased by ~20%, compared to that of control monolayers.

In the presence of dansylcadaverine or dynasore, flux of amidine-modified PNP (20 and 120 nm) decreased by ~85% compared to controls. On the other hand, flux of carboxylated PNP (20 and 100 nm) measured in the presence of dansylcadaverine or dynasore were not significantly different from respective controls (data not shown). Rt of MDCK-II treated with dansylcadaverine or dynasore decreased by ~50% and increased by ~50%, respectively, compared to those of control monolayers.

Figure 5 (Panels A and B) shows colocalization of intracellular amidine-modified 120 nm PNP with clathrin heavy chain after 1 h exposure to apical [PNP] of 176 μg/mL. When MDCK-II cells were co-incubated apically with 200 μM monodansylcadaverine and 120 nm positively charged PNP for 1 h and processed for confocal microscopy, very few amidine-modified 120 nm PNP were found inside the cells. The few PNP found intracellularly did not colocalize with clathrin heavy chain in these cells (Figure 5, Panel C).

Discussion

This study demonstrates that translocation of PNP across MDCK-II occurs transcellularly in a manner significantly dependent on surface charge. Positively charged PNP traverse MDCK-II via a clathrin-mediated pathway. The mechanism of PNP trafficking across epithelial monolayers (i.e., MDCK-II vs RAECM) appears to be highly cell type-specific.

We recently reported that cationic PNP (amidine-modified) are translocated across RAECM 20–40 times faster than anionic PNP (carboxyl-modified) [14]. By contrast, the trafficking rates of amidine-modified PNP across MDCK-II are 500 times faster than those of carboxyl-modified PNP. Negatively charged components (e.g., glycocalyx) on cell plasma membranes of epithelia may be at least in part responsible for promoting translocation of positively charged (but not negatively charged) NP, although titration of the membrane negative charge on RAECM caused only a relatively small decrease in amidine-modified PNP flux [13]. Harush-Frenkel et al [9] reported 2-fold greater uptake of cationic (polyethylene glycol)-D,L-polylactide (PEG-PLA; ~100 nm) NP in MDCK cells than that of comparably sized anionic PEG-PLA NP. Des Rieux et al [24] reported that amidine-coated polystyrene particles (200 nm) have higher hydrophobicity and translocate faster across intestinal epithelial cell monolayers (Caco-2 cells) than similarly sized carboxylate-coated polystyrene particles. Our laboratory reported that positively charged PNP are more hydrophobic than negatively charged PNP [13], which may have contributed to more rapid translocation of amidine-modified PNP through the lipid bilayers of RAECM plasma membranes.

Trafficking of small hydrophilic solutes across epithelial barriers can occur via paracellular pathways [25]. Although treatment of epithelial cells with EGTA (a calcium chelator) is reported to increase paracellular permeability by changing the distribution of a number of

tight and adherens junctional/cytoskeletal proteins [25,26,27,28], including redistribution of some of these proteins into intracellular compartments by clathrin-mediated endocytosis [29,30], it is unknown if NP traverse normal and/or EGTA-disrupted tight junctions. In this study, trafficking rates of PNP (small and large; positive and negative surface charge) across MDCK-II in the presence of 2 mM EGTA did not increase, indicating that these PNP do not traverse MDCK-II via tight junctional pathways under normal conditions or following EGTA treatment. The mechanism(s) responsible for the EGTA-induced decrease in flux of 120 nm (but not 20 nm) amidine-modified PNP are currently unknown, although we can speculate that the low extracellular Ca^{2+} might have altered formation of clathrin-coated pits. Trafficking rates of 20 and 100 nm carboxylate-modified PNP across MDCK-II do not appear to take place via endocytosis with or without EGTA treatment. These findings, along with localization of PNP predominantly in cytoplasm but not at cell-cell junctions, suggests that PNP cross MDCK-II via transcellular pathways. Yacobi et al [13] concluded that translocation of PNP across RAECM also takes place predominantly via transcellular pathways.

PNP trafficking was decreased by ~75% across MDCK-II when temperature was lowered from 37 to 4°C. In this regard, Dausend et al [7] reported uptake into HeLa cells of PNP (amino group- and cetyltrimethylammonium chloride-modified at particle surfaces with ~100 nm diameter) was decreased by ~60% at 4°C compared to that observed at 37°C. Guerriero et al [31] reported ~95% decrease in cellular ATP level after treating MDCK-II cells with 2% (10 mM) sodium azide. In this study, 10 mM sodium azide reduced trafficking rates of positively charged PNP by ~75% across MDCK-II. These data suggest that ATP/energy-dependent mechanism(s) may be involved in translocation of positively charged PNP across MDCK-II.

Methyl-β-cyclodextrin extracts cholesterol from plasma membranes and therefore inhibits lipid raft-mediated endocytosis (including caveolin-mediated endocytosis, CLIC/GEEC endocytosis, arf6-medited endocytosis, flotillin-mediated endocytosis and macropinocytosis [19,22]). Flux of PNP observed in the presence of 10–200 μM methyl-β-cyclodextrin did not decrease, suggesting that translocation of PNP across MDCK-II is not taking place via lipid raft-mediated endocytosis. Our laboratory has recently reported that translocation of PNP across RAECM was also not decreased in the presence of 10–200 μM methyl-β-cyclodextrin [13].

Involvement of clathrin-mediated endocytosis in uptake/translocation of various NP in cells and tissues (e.g., mesoporous silica nanoparticles in human mesenchymal stem cells [32], PEG-PLA NP into HeLa cells [8] and fullerenic NP into rat fibroblasts and rat hepatoma cells [33]) has been reported. Clathrin is composed of three light and three heavy chains that form a triskelion. Assembly of the triskelion leads to formation of a net-like basket (clathrin-coated pit) at the cell plasma membrane. The maximum diameter of clathrin-coated pits is ~100–150 nm [7]. Monodansylcadaverine has been widely used as an inhibitor of clathrin-mediated endocytosis, although its effects on macropinocytosis and phagocytosis remain controversial [22]. Monodansylcadaverine inhibits activity of transglutaminase (a key regulator of actin assembly and dynamics), as exemplified by inhibition of clathrin-mediated endocytosis of a number of ligands such as transferrin [22]. Treatment of MDCK-II with 200 μM monodansylcadaverine in our study led to ~80% decrease in trafficking rates of amidine-modified PNP (20 and 120 nm). It is of particular note that Harush-Frenkel et al [8,9] suggested a charge-dependent clathrin-mediated mechanism, in that uptake of positively (but not negatively) charged PEGylated D,L-polylactide (PLA) NP into HeLa and MDCK-II cells was demonstrated. In this regard, our data on much greater trafficking of positively charged (compared to that of negatively charged) PNP across MDCK-II may be governed by a similar charge-dependence of clathrin-mediated endocytosis. This

observation of clathrin-mediated trafficking of positively charged PNP across MDCK-II appears to be cell type-specific, since trafficking of the same PNP across RAECM does not take place via clathrin-mediated endocytosis [13]. In this study, confocal microscopy revealed colocalization of positively charged PNP with clathrin heavy chains in MDCK-II, while such colocalization was absent when the same experiments were performed in RAECM [13].

The large GTPase dynamin is a protein that self-assembles into a helical structure and wraps around the neck of newly formed cell plasma membrane invaginations to pinch them off from the cell plasma membrane, thus forming intracellular vesicles. Dynamin is essential for formation of caveolin- and clathrin-coated vesicles and plays a role in some lipid raft-mediated processes. Dynasore is a small cell permeable molecule that inhibits dynamin GTPase and rapidly blocks formation of these vesicles [34]. Our data showing that the presence of 80 μM dynasore in bathing fluids decreases trafficking rates of positively charged PNP across MDCK-II most likely reflects decreased trafficking via clathrin-mediated pathways. In HeLa cells, 80 μM dynasore inhibited uptake of positively charged PNP (~100 nm hydrodynamic diameter) 2-fold compared to that of negatively charged PNP of comparable size [7]. We reported recently that dynasore has no effect on trafficking rates of all types of PNP across RAECM, indicating that PNP trafficking across RAECM does not take place via endocytosis that requires dynamin activity [13].

In summary, we have shown that translocation of amidine-modified 20 and 120 nm PNP across MDCK-II occurs transcellularly, requires cellular energy and involves clathrin/dynamin-dependent endocytosis. Higher trafficking rates of amidine-modified PNP compared to those of carboxylate-modified PNP of similar size across MDCK-II may be related to the charge-selective behavior of clathrin-mediated endocytosis. By contrast, none of the PNP was reported to traverse RAECM via endocytic mechanisms [13,14]. We conclude that NP interactions with particular epithelial barriers are dependent on both physicochemical properties of NP and specific (epithelial) cell types.

Acknowledgments

Contract grant sponsor: Hastings Foundation, Whittier Foundation and National Institutes of Health Research Grants DK062283, EY011386, EY017923, ES017034, ES018782, HL038621, HL038658, HL062569 and HL089445.

List of abbreviated terms

MDCK	Madin Darby Canine Kidney cell monolayers
MDCK-II	type II MDCK
PNP	polystyrene nanoparticles
MBC	methyl-β-cyclodextrin
NP	nanoparticles
RAECM	rat alveolar epithelial cell monolayers
DME	Dulbecco’s modified Eagle’s medium
Rt	transmonolayer electrical resistance
EGTA	ethylene glycol-bis-(2-aminoethyl)-N,N,N′,N′-tetraacetic acid
TX-100	Triton X-100
ZO-1	zonula occludens-1

DAPI	4′,6-diamidino-2-phenylindole
PEG-PLA	polyethylene glycol-D,L-polylactide

References

1. Farokhzad OC, Langer R. Impact of nanotechnology on drug delivery. ACS Nano. 2009; 3:16–20. [PubMed: 19206243]
2. Card JW, Zeldin DC, Bonner JC, Nestmann ER. Pulmonary applications and toxicity of engineered nanoparticles. Am J Physiol Lung Cell Mol Physiol. 2008; 295:L400–L411. [PubMed: 18641236]
3. Xia T, Kovochich M, Liong M, Zink JI, Nel AE. Cationic polystyrene nanosphere toxicity depends on cell-specific endocytic and mitochondrial injury pathways. ACS Nano. 2008; 2:85–96. [PubMed: 19206551]
4. Cuenca AG, Jiang H, Hochwald SN, Delano M, Cance WG, Grobmyer SR. Emerging implications of nanotechnology on cancer diagnostics and therapeutics. Cancer. 2006; 107:459–66. [PubMed: 16795065]
5. Freitas RA Jr. Nanotechnology, nanomedicine and nanosurgery. Int J Surg. 2005; 3:243–46. [PubMed: 17462292]
6. Yacobi NR, Phuleria HC, Demaio L, Liang CH, Peng CA, Sioutas C, et al. Nanoparticle effects on rat alveolar epithelial cell monolayer barrier properties. Toxicol In Vitro. 2007; 21:1373–81. [PubMed: 17555923]
7. Dausend J, Musyanovych A, Dass M, Walther P, Schrezenmeier H, Landfester K, et al. Uptake mechanism of oppositely charged fluorescent nanoparticles in hela cells. Macromol Biosci. 2008; 8:1135–43. [PubMed: 18698581]
8. Harush-Frenkel O, Debotton N, Benita S, Altschuler Y. Targeting of nanoparticles to the clathrin-mediated endocytic pathway. Biochem Biophys Res Commun. 2007; 353:26–32. [PubMed: 17184736]
9. Harush-Frenkel O, Rozentur E, Benita S, Altschuler Y. Surface charge of nanoparticles determines their endocytic and transcytotic pathway in polarized MDCK cells. Biomacromolecules. 2008; 9 : 435–43. [PubMed: 18189360]
10. Hansen CG, Nichols BJ. Molecular mechanisms of clathrin-independent endocytosis. J Cell Sci. 2009; 122:1713–21. [PubMed: 19461071]
11. Geiser M, Rothen-Rutishauser B, Kapp N, Schurch S, Kreyling W, Schulz H, et al. Ultrafine particles cross cellular membranes by nonphagocytic mechanisms in lungs and in cultured cells. Environ Health Perspect. 2005; 113:1555–60. [PubMed: 16263511]
12. Rejman J, Oberle V, Zuhorn IS, Hoekstra D. Size-dependent internalization of particles via the pathways of clathrin- and caveolae-mediated endocytosis. Biochem J. 2004; 377:159–69. [PubMed: 14505488]
13. Yacobi NR, Malmstadt N, Fazlollahi F, Demaio L, Marchelletta R, Hamm-Alvarez SF, et al. Mechanisms of alveolar epithelial translocation of a defined population of nanoparticles. Am J Respir Cell Mol Biol. 2010; 42:604–14. [PubMed: 19574531]
14. Yacobi NR, Demaio L, Xie J, Hamm-Alvarez SF, Borok Z, Kim KJ, et al. Polystyrene nanoparticle trafficking across alveolar epithelium. Nanomedicine. 2008; 4:139–45. [PubMed: 18375191]
15. Angelow S, Kim KJ, Yu AS. Claudin-8 modulates paracellular permeability to acidic and basic ions in MDCK II cells. J Physiol. 2006; 571:15–26. [PubMed: 16322055]
16. Angelow S, Schneeberger EE, Yu AS. Claudin-8 expression in renal epithelial cells augments the paracellular barrier by replacing endogenous claudin-2. J Membr Biol. 2007; 215:147–59. [PubMed: 17516019]
17. Lei L, Sun H, Liu D, Liu L, Li S. Transport of val-leu-pro-val-pro in human intestinal epithelial (caco-2) cell monolayers. J Agric Food Chem. 2008; 56:3582–86. [PubMed: 18442243]
18. Parton RG, Richards AA. Lipid rafts and caveolae as portals for endocytosis: New insights and common mechanisms. Traffic. 2003; 4:724–738. [PubMed: 14617356]

19. Doherty GJ, McMahon HT. Mechanisms of endocytosis. Annu Rev Biochem. 2009; 78:857–902. [PubMed: 19317650]
20. Wang LH, Rothberg KG, Anderson RG. Mis-assembly of clathrin lattices on endosomes reveals a regulatory switch for coated pit formation. J Cell Biol. 1993; 123:1107–17. [PubMed: 8245121]
21. Davies PJ, Cornwell MM, Johnson JD, Reggianni A, Myers M, Murtaugh MP. Studies on the effects of dansylcadaverine and related compounds on receptor-mediated endocytosis in cultured cells. Diabetes Care. 1984; 7:35–41. [PubMed: 6145551]
22. Ivanov AI. Pharmacological inhibition of endocytic pathways: Is it specific enough to be useful? Methods Mol Biol. 2008; 440:15–33. [PubMed: 18369934]
23. Kirchhausen T, Macia E, Pelish HE. Use of dynasore, the small molecule inhibitor of dynamin, in the regulation of endocytosis. Methods Enzymol. 2008; 438:77–93. [PubMed: 18413242]
24. Rieux A, Ragnarsson EG, Gullberg E, Preat V, Schneider YJ, Artursson P. Transport of nanoparticles across an in vitro model of the human intestinal follicle associated epithelium. Eur J Pharm Sci. 2005; 25:455–65. [PubMed: 15946828]
25. Collares-Buzato CB, McEwan GT, Jepson MA, Simmons NL, Hirst BH. Paracellular barrier and junctional protein distribution depend on basolateral extracellular ca2+ in cultured epithelia. Biochim Biophys Acta. 1994; 1222:147–58. [PubMed: 8031850]
26. Mounier J, Vasselon T, Hellio R, Lesourd M, Sansonetti PJ. Shigella flexneri enters human colonic caco-2 epithelial cells through the basolateral pole. Infect Immun. 1992; 60:237–48. [PubMed: 1729185]
27. Knipp GT, Ho NF, Barsuhn CL, Borchardt RT. Paracellular diffusion in caco-2 cell monolayers: Effect of perturbation on the transport of hydrophilic compounds that vary in charge and size. J Pharm Sci. 1997; 86:1105–10. [PubMed: 9344165]
28. Sergent T, Parys M, Garsou S, Pussemier L, Schneider YJ, Larondelle Y. Deoxynivalenol transport across human intestinal caco-2 cells and its effects on cellular metabolism at realistic intestinal concentrations. Toxicol Lett. 2006; 164:167–76. [PubMed: 16442754]
29. Giepmans BN, van Ijzendoorn SC. Epithelial cell-cell junctions and plasma membrane domains. Biochim Biophys Acta. 2009; 1788:820–31. [PubMed: 18706883]
30. Ivanov AI, Nusrat A, Parkos CA. Endocytosis of epithelial apical junctional proteins by a clathrin-mediated pathway into a unique storage compartment. Mol Biol Cell. 2004; 15:176–88. [PubMed: 14528017]
31. Guerriero CJ, Weisz OA. N-wasp inhibitor wiskostatin nonselectively perturbs membrane transport by decreasing cellular ATP levels. Am J Physiol Cell Physiol. 2007; 292:1562–66.
32. Huang DM, Hung Y, Ko BS, Hsu SC, Chen WH, Chien CL, et al. Highly efficient cellular labeling of mesoporous nanoparticles in human mesenchymal stem cells: Implication for stem cell tracking. Faseb J. 2005; 19:2014–16. [PubMed: 16230334]
33. Li W, Chen C, Ye C, Wei T, Zhao Y, Lao F, et al. The translocation of fullerenic nanoparticles into lysosome via the pathway of clathrin-mediated endocytosis. Nanotechnology. 2008; 19:145102–114. [PubMed: 21817752]
34. Macia E, Ehrlich M, Massol R, Boucrot E, Brunner C, Kirchhausen T. Dynasore, a cell-permeable inhibitor of dynamin. Dev Cell. 2006; 10:839–50. [PubMed: 16740485]

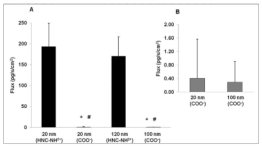

Figure 1.

Flux of PNP (amidine-modified 20 and 120 nm (panel A) and carboxylate-modified 20 and 100 nm (panel B)) across MDCK-II at apical [PNP] of 176 μg/mL (n = 14–21). * = significantly different from 20 nm amidine-modified PNP fluxes. # = significantly different from 120 nm amidine-modified PNP fluxes.

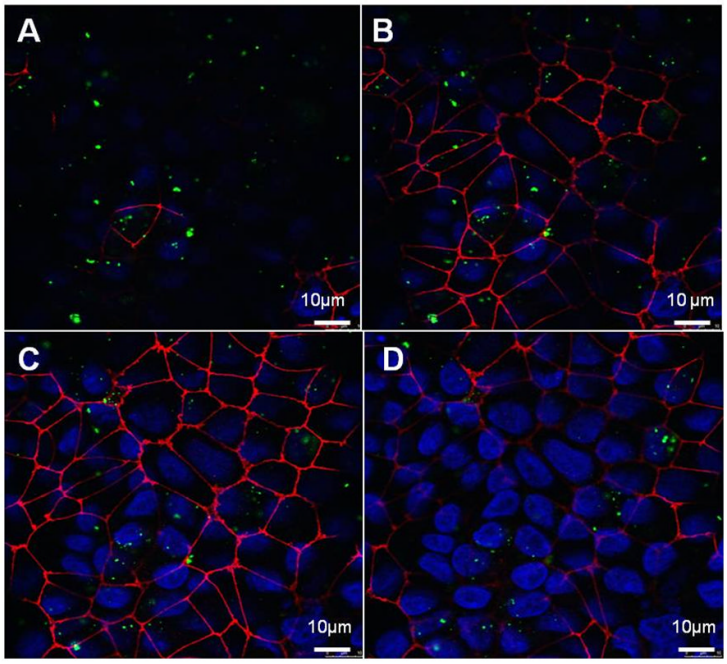

Figure 2.

Confocal images of MDCK-II exposed at 37°C apically to PNP (120 nm amidine-modified at 176 μg/mL) for 24 h. Panels A through D: Planar cross-sections of MDCK-II at 1 μm vertical intervals from apical (A) to basolateral (D) aspects. Cell borders are stained red, nuclei are stained blue and PNP appear green. PNP are observed generally in cytoplasm inside cells and not in cell-cell junctions or nuclei.

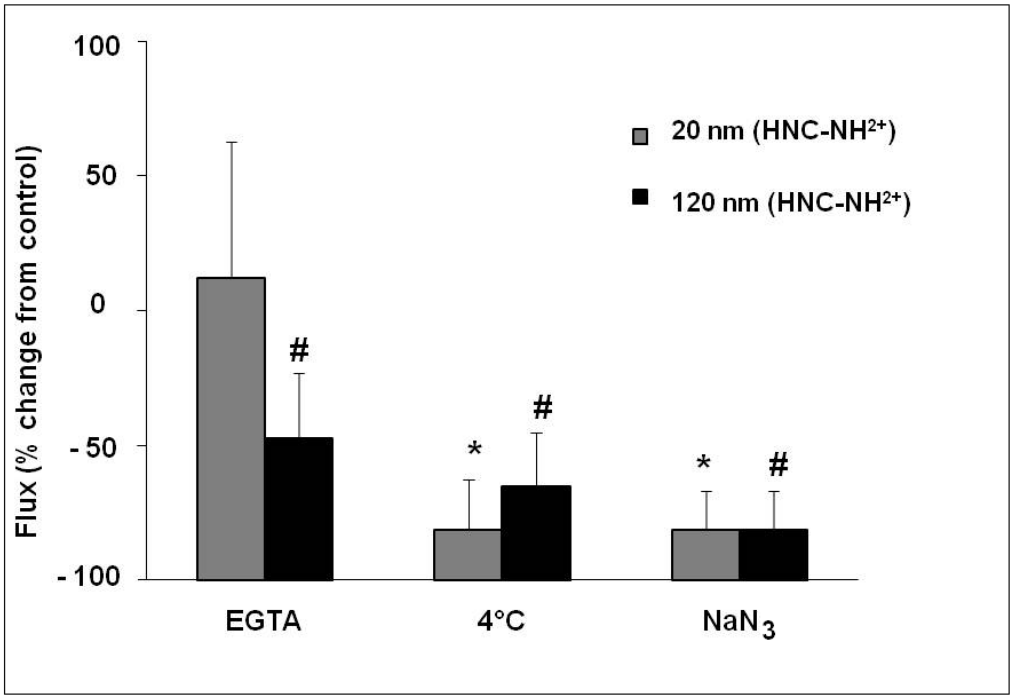

Figure 3.

Effects of 2 mM EGTA, decreased temperature and cellular energy depletion on flux of PNP (amidine-modified 20 and 120 nm) at an apical concentration of 176 μg/mL across MDCK-II. Monolayers treated with 2 mM EGTA did not exhibit increased PNP fluxes compared to no EGTA control (n=6). At 4 °C, PNP flux decreased ~75% compared to 37°C control (n = 6–7). PNP flux across monolayers treated with 10 mM NaN_3 decreased ~80% compared to no NaN_3 control (n=6–9). * = significantly different from 20 nm, amidine-modified control. # = significantly different from 120 nm, amidine-modified control.

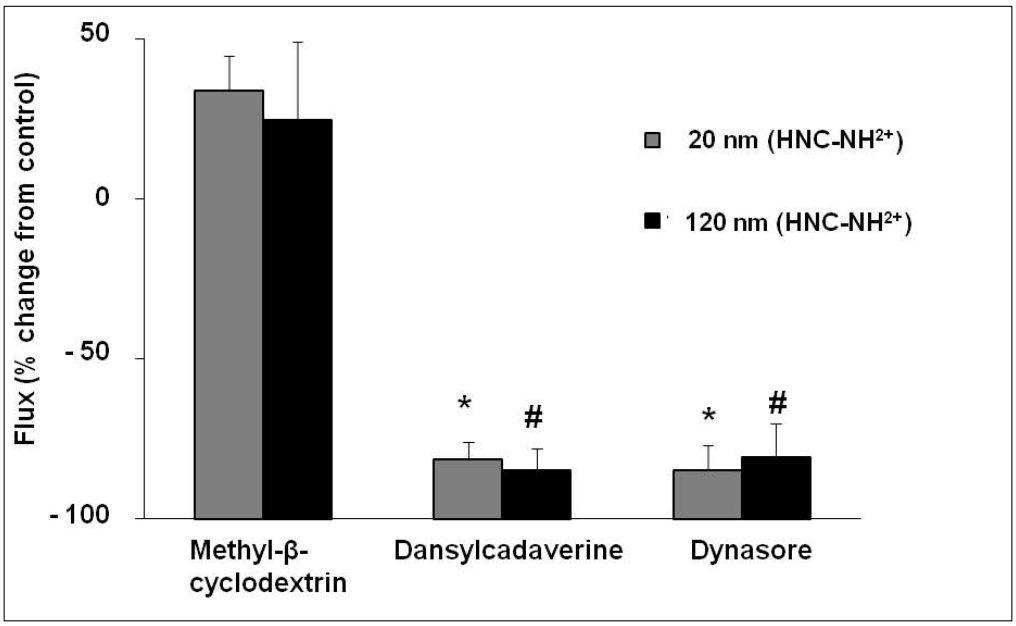

Figure 4.

Effects of inhibition of lipid raft-mediated, clathrin-mediated and dynamin-dependent endocytosis on flux of PNP (amidine-modified 20 and 120 nm) at an apical concentration of 176 μg/mL across MDCK-II. Monolayers treated with 10 μM methyl-β-cyclodextrin did not exhibit decreased PNP flux (n=6). Monolayers treated with either 200 μM dansylcadaverine or 80 μM dynasore, respectively, showed markedly decrease in PNP flux (n=6–9). * = significantly different from 20 nm, amidine-modified control. # = significantly different from 120 nm, amidine-modified control.

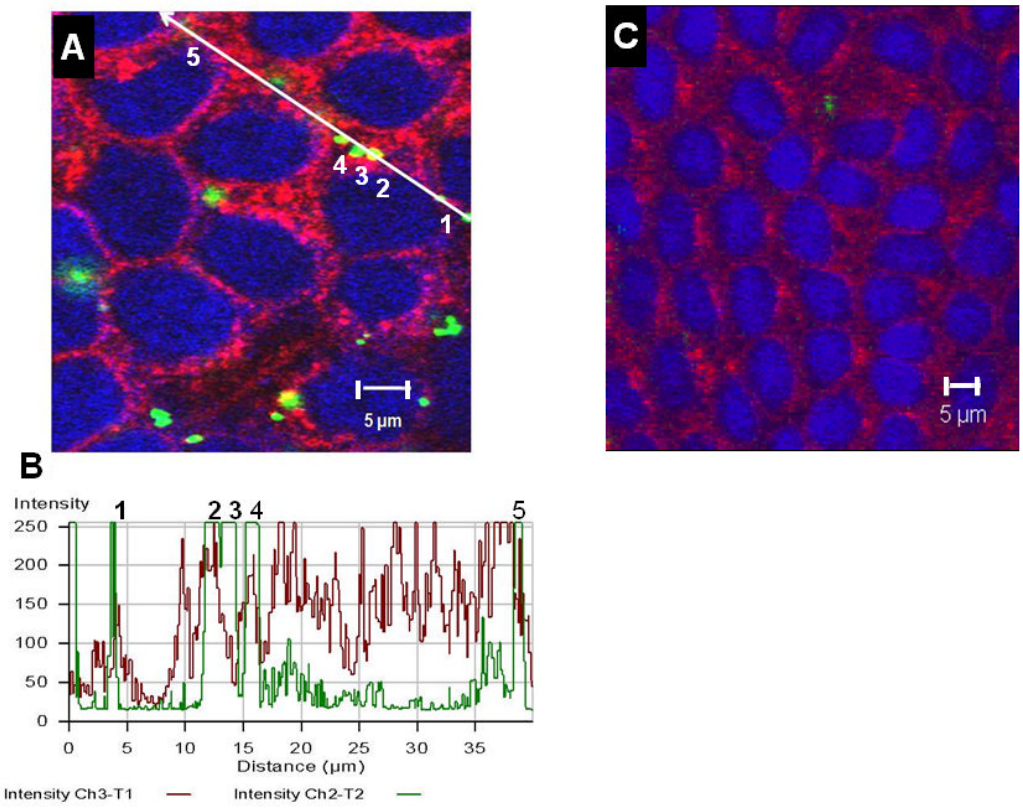

Figure 5.

Confocal photomicrographs demonstrating internalized PNP (120 nm amidine-modified) and clathrin heavy chain in MDCK-II after 1 h of apical exposure to 176 μg/mL PNP in the absence of dansylcadaverine (Panel A). PNP appear in green, nuclei in blue and clathrin heavy chain in red. PNP colocalizes with clathrin heavy chain, appearing yellowish-green. Panel B illustrates the colocalization profile of PNP (green) and clathrin heavy chain (red), where color intensities from green and red channels are estimated along the line segment shown in panel A. As can be appreciated, green intensity peaks coincide with red intensity peaks. The numbers 1–5 in panel B correspond to those in panel A, respectively. Panel C represents a typical confocal image obtained from MDCK-II co-incubated apically with 200 μM dansylcadaverine and 120 nm amidine-modified PNP for 1 h. Comparatively few PNP (green) can be seen in Panel C. No colocalization of PNP and clathrin heavy chain (red) is detectable in Panel C.